Liquid Crystals
Publication details, including instructions for authors and subscription information:
http://www.informaworld.com/smpp/title~content=t713926090

Structures of two crystal forms of chiral smectogenic 4'-hexyloxy-4-biphenylyl *p*-[(*S*)-2-methylbuty 1] benzoate

Kayako Hori[a]; Yuji Ohashi[b]
[a] Department of Chemistry, Ochanomizu University, Tokyo, Japan [b] Department of Chemistry, Tokyo Institute of Technology, Tokyo, Japan

To cite this Article Hori, Kayako and Ohashi, Yuji(1991) 'Structures of two crystal forms of chiral smectogenic 4'-hexyloxy-4-biphenylyl *p*-[(*S*)-2-methylbuty 1] benzoate', Liquid Crystals, 9: 3, 383 — 396
To link to this Article: DOI: 10.1080/02678299108045572
URL: http://dx.doi.org/10.1080/02678299108045572

LIQUID CRYSTALS, 1991, VOL. 9, NO. 3, 383–396

Structures of two crystal forms of chiral smectogenic 4′-hexyloxy-4-biphenylyl *p*-[(*S*)-2-methylbutyl]benzoate

by KAYAKO HORI*
Department of Chemistry, Ochanomizu University, Otsuka, Bunkyo-ku, Tokyo 112, Japan

and YUJI OHASHI
Department of Chemistry, Tokyo Institute of Technology, O-okayama, Meguro-ku, Tokyo 152, Japan

(*Received 11 July 1990; accepted 15 September 1990*)

Three crystal forms were found for the title compound. The relationship of the polymorphs was elucidated by DSC and powder X-ray diffraction methods. Two crystal structures, stable at room temperature, have been determined by single crystal X-ray analysis. Crystal data: 4′-hexyloxy-4-biphenylyl *p*-[(*S*)-2-methylbutyl]benzoate,

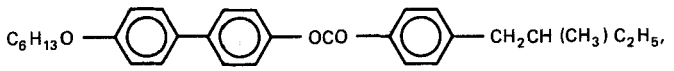

$M_r = 444{\cdot}6$, $C_{30}H_{36}O_3$, **1**, triclinic, P1, $T = 298$ K, $a = 11{\cdot}550(2)$, $b = 22{\cdot}940(3)$, $c = 11{\cdot}810(3)$ Å, $\alpha = 104{\cdot}08(2)$, $\beta = 112{\cdot}87(2)$, $\gamma = 99{\cdot}49(2)°$, $V = 2676(1)$ Å^3, $d_x = 1{\cdot}110$ g cm^{-3}, $\mu = 4{\cdot}74$ cm^{-1}, $F(000) = 960$; **2**, monoclinic, $P2_1$, $T = 298$ K, $a = 23{\cdot}304(2)$, $b = 5{\cdot}6080(5)$, $c = 20{\cdot}451(4)$ Å, $\beta = 98{\cdot}39(1)°$, $V = 2644{\cdot}1(6)$ Å^3, $Z = 4$, $d_x = 1{\cdot}117$ g cm^{-3}, $\mu = 4{\cdot}80$ cm^{-1}, $F(000) = 960$. Each crystal is composed of a smectic-like layer structure with a large molecular tilt angle (45° and 60°, respectively). The molecules in **1** have largely twisted paraffin chains and the twisted biphenyl moieties, while those in **2** have all-trans zigzag paraffin chains and coplanar biphenyl moieties. Packing modes of the core moieties are also largely different: some of the mutual arrangements of the phenyl rings are nearly parallel (~20°) in **1**, while the contact angle of the phenyl rings between the neighbouring molecules is 60° on average in **2**.

1. Introduction

Chiral smectic phases are receiving a great deal of attention because of the ferroelectricity. Intermolecular interactions controlling the phases, however, have not been sufficiently elucidated at molecular level. In order to find relationship between the mesophase behaviour and intermolecular interactions revealed in crystal structures, systematic single crystal structure analyses have been carried out for three isomeric series of biphenyl esters with various mesophase characteristics. In the crystals of the first series, *p*-pentyloxyphenyl and *p*-heptyloxyphenyl 4′-[(*S*)-2-methylbutyl]biphenyl-4-carboxylates (I-5 and I-7, respectively), which have a S_C^* followed by a cholesteric [1], paraffin chains have close contacts between layers [2], while in the second series, *p*-[(*S*)-2-methylbutyl]phenyl 4′-heptyloxybiphenyl-4-carboxylate and 4′-octyloxybiphenyl-4-carboxylate (II-7 and II-8, respectively), which

* Author for correspondence.

0267–8292/91 $3·00

transform to a S_C^* and then to a S_A, whole molecules including paraffin chains contribute to the lateral overlapping within a layer [3].

For the third series, 4′-alkoxy-4-biphenylyl *p*-[(*S*)-2-methylbutyl]benzoates, two crystal forms were found for the heptyl homologue (III-7M for the monoclinic crystal and III-7T for the triclinic one), which transform to S_I^* and S_J^*, respectively. The paraffin chains of the parallel molecules in III-7M have close contacts within a layer, being interpreted to cause the transition to the higher ordered smectic (S_I^*) than S_C^* [4]. Sufficient data, however, have not been obtained for III-7T due to the poor crystallinity. For the hexyl homologue of the third series, two forms of single crystals, triclinic and monoclinic, were obtained (III-6T and III-6M, respectively). III-6T is approximately isomorphous to III-7T. Both crystals, III-6T and III-6M, transform to the same high-temperature crystalline phase. This paper describes the polymorphism and the crystal structures of III-6T and III-6M.

2. Experimental

Compound. 4′-Hexyloxy-4-biphenylyl *p*-[(*S*)-2-methylbutyl]benzoate was synthesized and purified as reported previously [4].

Apparatus. Transition temperatures were measured using a Seiko SSC570 DSC and an Olympus POM polarizing microscope equipped with a Mettler FP 82 hotstage. Powder X-ray diffraction patterns were obtained using Rigaku Geigerflex 2001 with a Cu Kα radiation.

Crystal structure analysis. Transparent flat plate-like or long parallelepiped crystals were separately grown from a methanol–chloroform solution. Oscillation and Weissenberg photographs showed that they belong to triclinic (III-6T) and monoclinic (III-6M) systems, respectively. Data collection procedures are summarized in table 1.

The structures were determined by applying the program MULTAN78 [5] and refined by loosely constrained block-matrix least-squares using SHELX76 [6]. The quantity minimized was $\Sigma w(|F_o|-|F_c|)^2$, where $w=(\sigma(|F_o|)^2+0{\cdot}004|F_o|^2)^{-1}$. Atomic scattering factors were taken from *International Tables for X-ray Crystallography* [7].

Table 1. Experimental conditions.

	III-6T	III-6M
X-ray source	Cu Kα monochromated by graphite ($\lambda=1{\cdot}54184$ Å)	
Diffractometer	Rigaku AFC-4	
L.s. for cell const.	19 refl. ($47<2\theta<53°$)	17 refl. ($31<2\theta<53°$)
Scan mode	$2\theta-\omega$	
2θ range	$3°<2\theta<125°$	
Scan width	$\omega=(1{\cdot}0+0{\cdot}15\tan\theta)°$	
Scan rate/°(2θ) min^{-1}	8 ($2\theta<85°$) 4 ($2\theta>85°$)	8
Backgrounds	5 s at both ends of a scan	
Standard reflections	Three after every 50 reflections	
Intensity variation	Not significant	
Crystal size/mm	$0{\cdot}5\times0{\cdot}3\times0{\cdot}05$	$0{\cdot}4\times0{\cdot}2\times0{\cdot}02$
Total number of refl.	7624	4549
Number of refl. ($>3\sigma(\|F_o\|)$)	4276	2861
Correction	Lp but not for absorption	

In the course of refinement of III-6T, additional peaks were found around the paraffin chains and chiral groups, whose temperature factors were remarkably large. These peaks were included as disordered atoms in further refinements. Some of the atoms in the chains, however, still have large temperature factors, in spite of no significant peaks around them. Besides, it was very difficult to obtain appropriate geometries for these disordered atoms, especially for those with minor occupancies. These facts are considered to be due to the highly disordered chains. But, such a disordered structure is represented by only two conformers for each molecule in order not to increase greatly the number of the parameters. Thus, the occupation factors were given to make the temperature factors of the different conformers similar and were fixed in further refinements. For III-6M, terminal atoms of the chiral groups are disordered. All the non-hydrogen atoms except for the disordered atoms were refined anisotropically. Only 19 (III-6T) and 26 (III-6M) hydrogen atoms found in the difference Fourier maps were included in the refinement, because of the limited number of reflections due to the large thermal effect. Max Δ/σ and max $\Delta\rho$ in the final refinement were 0·46 and 0·29 e Å^{-3} for III-6T, and 0·34 and 0·26 e Å^{-3} for III-6M. Final $R(R_w)$ values were 0·119 (0·128) and 0·100 (0·113), respectively. The large value of the former is due to the highly disordered structure. The final coordinates of non-hydrogen atoms are given in tables 2 and 3 [8]. Computations were carried out on an IBM 4381-R24 computer at the Computer Centre of Ochanomizu University.

Table 2. Final atomic coordinates with their estimated standard deviations, multiplied by 10^4 for III-6T.

Atom	x	y	z	B_{eq}/Å^2†
O(1A)	10893(7)	3023(4)	4475(9)	10·5
O(2A)	8836	2478	3455	10·5
O(3A)	10091(11)	−888(5)	−2513(10)	12·1
C(1A)	9782(15)	−423(6)	−1817(11)	9·9
C(2A)	10092(14)	−421(6)	−598(12)	9·7
C(3A)	10031(13)	56(6)	339(10)	8·8
C(4A)	9531(11)	539(5)	−29(9)	8·2
C(5A)	9167(13)	506(6)	−1313(11)	8·7
C(6A)	9313(17)	42(6)	−2181(11)	10·6
C(7A)	9337(10)	1061(5)	857(10)	6·6
C(8A)	9228(11)	988(5)	1977(11)	7·4
C(9A)	9088(13)	1463(6)	2834(12)	8·2
C(10A)	8983(12)	2003(5)	2522(14)	9·5
C(11A)	9008(16)	2082(7)	1411(13)	12·1
C(12A)	9288(14)	1632(6)	670(12)	9·3
C(13A)	9823(8)	2985(5)	4334(9)	5·2
C(14A)	9478(12)	3486(7)	5065(12)	7·9
C(15A)	10447(15)	4002(6)	6021(14)	9·8
C(16A)	10120(16)	4467(6)	6743(14)	10·4
C(17A)	8825(17)	4409(7)	6529(16)	12·3
C(18A)	7878(14)	3854(9)	5655(18)	13·2
C(19A)	8210(13)	3397(7)	4934(16)	12·7
C(21A)	8559(17)	4904(8)	7379(16)	12·7
C(22A)	8590(25)	4826(11)	8647(18)	18·2
C(23A)	8248(52)	5365(16)	9379(38)	20·2(21)‡
C(23A′)	7877(41)	4219(19)	8777(38)	11·8(11)‡
C(24A)	9331(52)	5982(12)	9915(50)	26·2(20)‡
C(24A′)	7572(71)	4932(36)	9262(67)	20·3(24)‡

Table 2 (*continued*).

Atom	*x*	*y*	*z*	B_{eq}/Å^2)†
C(25A)	9195(45)	4357(18)	9056(33)	21·0(15)‡
C(25A′)	8630(138)	5467(51)	9660(118)	23·3(41)‡
C(31A)	9879(24)	−877(11)	−3791(16)	19·5
C(32A)	10767(32)	−1250(12)	−4113(30)	28·1
C(33A)	9699(26)	−1869(15)	−4936(32)	15·9(11)‡
C(33A′)	10647(43)	−1718(20)	−4143(42)	8·2(9)‡
C(34A)	10338(39)	−2388(13)	−5322(35)	19·7‡
C(34A′)	11129(31)	−2266(14)	−5429(28)	9·8(43)‡
C(35A)	10355(37)	−2620(18)	−6618(34)	19·7‡
C(35A′)	11203(100)	−2054(46)	−4836(97)	19·7‡
C(36A)	11564(36)	−2870(18)	−6425(35)	19·7‡
C(36A′)	10567(97)	−3301(46)	−6690(89)	19·7‡
O(1B)	7274(13)	−1095(5)	3265(12)	12·0
O(2B)	7483(8)	−409(4)	2254(8)	8·6
O(3B)	7020(8)	2711(4)	9309(9)	9·6
C(1B)	6949(14)	2251(6)	8265(10)	7·0
C(2B)	6004(14)	1678(8)	7519(12)	10·2
C(3B)	6081(13)	1248(6)	6523(13)	12·1
C(4B)	7182(11)	1371(6)	6306(10)	6·9
C(5B)	8174(14)	1944(7)	7113(15)	9·9
C(6B)	8077(14)	2369(5)	8115(13)	8·3
C(7B)	7291(12)	899(7)	5245(13)	10·8
C(8B)	8578(12)	861(5)	5453(13)	8·8
C(9B)	8634(11)	405(6)	4457(12)	7·4
C(10B)	7555(11)	60(5)	3300(11)	6·2
C(11B)	6316(12)	123(5)	3083(10)	7·6
C(12B)	6238(11)	587(6)	4032(11)	7·9
C(13B)	7346(22)	−1002(8)	2317(18)	14·7
C(14B)	7507(12)	−1423(5)	1310(11)	7·6
C(15B)	7412(18)	−2052(7)	1239(17)	13·5
C(16B)	7556(16)	−2470(6)	272(13)	10·2
C(17B)	7755(12)	−2281(5)	−695(10)	8·4
C(18B)	7740(18)	−1703(6)	−766(15)	12·9
C(19B)	7660(13)	−1259(5)	279(12)	9·2
C(21B)	7960(20)	−2756(7)	−1612(14)	14·2
C(22B)	6854(25)	−3023(12)	−2988(21)	25·9
C(23B)	5710(25)	−3363(16)	−2833(29)	27·2
C(24B)	4508(32)	−3704(11)	−4216(23)	20·9
C(25B)	7367(22)	−3381(11)	−3913(20)	18·3
C(31B)	6014(15)	2588(9)	9720(16)	14·4
C(32B)	6393(19)	3065(12)	11075(20)	17·6
C(33B)	5879(37)	3604(12)	10770(23)	26·0
C(34B)	6488(30)	4170(10)	12094(27)	25·4
C(35B)	5490(26)	4152(12)	12638(19)	22·2
C(36B)	5871(24)	4786(8)	13708(21)	16·0
O(1C)	4340(10)	3805(4)	4841(8)	11·5
O(2C)	3999(9)	3064(4)	5697(7)	8·9
O(3C)	4585(12)	−48(5)	−1276(9)	12·8
C(1C)	4514(14)	417(7)	−350(14)	10·2
C(2C)	3435(12)	257(7)	−87(13)	9·8
C(3C)	3339(10)	706(5)	891(10)	6·8
C(4C)	4346(12)	1266(4)	1654(10)	8·6
C(5C)	5470(11)	1371(5)	1471(11)	7·5
C(6C)	5559(11)	944(5)	439(12)	7·8
C(7C)	4211(10)	1705(3)	2738(9)	5·0

Table 2 (*continued*).

Atom	*x*	*y*	*z*	B_{eq}/Å²†
C(8C)	3069(10)	1884(5)	2557(10)	6·9
C(9C)	3037(14)	2333(6)	3584(13)	8·4
C(10C)	4197(15)	2645(6)	4733(14)	11·8
C(11C)	5346(13)	2459(6)	4950(13)	8·9
C(12C)	5359(12)	2024(5)	3912(13)	9·6
C(13C)	4175(8)	3662(5)	5686(8)	5·1
C(14C)	4056(13)	4092(6)	6758(11)	10·1
C(15C)	3980(12)	3928(6)	7810(11)	8·5
C(16C)	3757(12)	4391(6)	8692(10)	10·0
C(17C)	3961(20)	5024(6)	8736(20)	16·4
C(18C)	3883(22)	5153(10)	7576(18)	17·0
C(19C)	4084(14)	4702(5)	6695(10)	8·7
C(21C)	3539(20)	5353(8)	9802(18)	15·9
C(22C)	4765(17)	5728(7)	11032(14)	12·1
C(23C)	4693(25)	6267(10)	12043(23)	20·7
C(25C)	5925(24)	6113(12)	11036(20)	20·1
C(24C)	3555(33)	5902(15)	12155(34)	19·4(13)‡
C(24C′)	3178(81)	6129(36)	11446(75)	15·8(22)‡
C(31C)	5802(15)	31(8)	−1338(17)	12·9
C(32C)	5904(35)	−598(13)	−2089(27)	12·7(10)‡
C(32C′)	5878(55)	−611(22)	−3047(57)	13·4(13)‡
C(33C)	4826(35)	−816(16)	−3479(30)	16·6(11)‡
C(33C′)	5133(53)	−857(21)	−2560(53)	10·8(11)‡
C(34C)	4905(30)	−1439(14)	−4388(29)	13·4(8)‡
C(34C′)	5861(71)	−911(33)	−3852(75)	19·7(23)‡
C(35C)	6198(32)	−1508(19)	−4439(40)	15·6(22)‡
C(35C′)	5945(55)	−1398(26)	−4329(52)	11·0(17)‡
C(36C)	5656(29)	−2102(13)	−5670(26)	10·4(7)‡
C(36C′)	6454(47)	−2091(19)	−5602(40)	11·8(12)‡
O(1D)	647(15)	−278(7)	3568(14)	15·5
O(2D)	2816(9)	177(4)	4607(9)	9·2
O(3D)	1500(10)	3566(4)	10547(9)	11·1
C(1D)	1651(12)	3075(6)	9705(13)	8·6
C(2D)	1442(12)	3055(7)	8446(13)	9·4
C(3D)	1696(13)	2611(5)	7612(15)	9·3
C(4D)	2162(10)	2150(5)	8087(11)	7·0
C(5D)	2342(17)	2145(7)	9327(12)	11·7
C(6D)	2193(17)	2630(8)	10197(15)	12·4
C(7D)	2261(11)	1621(6)	7118(12)	8·0
C(8D)	2153(16)	1690(8)	5942(12)	11·6
C(9D)	2383(15)	1209(7)	5146(16)	11·3
C(10D)	2503(12)	652(7)	5361(11)	8·7
C(11D)	2562(12)	590(5)	6527(13)	8·2
C(12D)	2472(12)	1089(6)	7426(12)	8·7
C(13D)	1736(18)	−281(8)	3712(17)	12·7
C(14D)	2153(14)	−732(6)	2869(13)	8·3
C(15D)	1194(14)	−1276(9)	1984(16)	11·8
C(16D)	1447(16)	−1759(7)	1241(15)	12·2
C(17D)	2764(16)	−1691(7)	1459(11)	9·8
C(18D)	3763(13)	−1164(7)	2464(14)	10·5
C(19D)	3487(14)	−694(6)	3248(12)	9·6
C(21D)	3202(25)	−2161(9)	633(18)	15·4
C(22D)	2644(23)	−2166(11)	−821(21)	22·5
C(23D)	2884(33)	−2781(14)	−1490(34)	19·7‡
C(23D′)	1630(97)	−2848(42)	−1185(89)	19·7‡

Table 2 (*continued*).

Atom	x	y	z	B_{eq}/Å^2†
C(24D)	1739(34)	−3373(15)	−2001(35)	19·7‡
C(24D′)	4258(89)	−1517(42)	−433(86)	19·7‡
C(25D)	3449(25)	−1516(12)	−652(27)	13·1(8)‡
C(25D′)	2534(92)	−3038(42)	1861(92)	19·7‡
C(31D)	1719(18)	3565(7)	11829(13)	12·2
C(32D)	1044(32)	4038(12)	12337(25)	21·3
C(33D)	1566(36)	4658(16)	12256(37)	17·4(13)‡
C(33D′)	699(48)	4193(24)	12877(49)	14·5(15)‡
C(34D)	1035(43)	5134(18)	12977(40)	18·1(15)‡
C(34D′)	12(73)	5016(34)	12811(69)	19·7‡
C(35D)	721(39)	5024(17)	14070(34)	15·7(12)‡
C(35D′)	−325(61)	4815(27)	13501(64)	16·7(19)‡
C(36D)	476(41)	5561(16)	14970(37)	16·1(12)‡
C(36D′)	−433(43)	5548(20)	14305(42)	11·9(11)‡

† $B_{eq}=(4/3)\sum_{ij}\beta_{ij}(\mathbf{a}_i\cdot\mathbf{a}_j)$.

‡ Isotropic temperature factors. The values without ESD were fixed. Occupation factors were fixed at 0·6 for C(23A)–C(25A), C(32C)–C(36C) and C(33D)–C(36D), 0·4 for their counterparts, 0·7 for C(33A)–C(36A), C(24C), C(23D)–C(25D), 0·3 for their counterparts.

Table 3. Final atomic coordinates with their estimated standard deviations, multiplied by 10^4 for III-6M.

Atom	x	y	z	B_{eq}/Å^2†
O(1A)	7848(3)	−2866(13)	1205(3)	8·6
O(2A)	7740(2)	456	1764(2)	6·2
O(3A)	3498(2)	1258(11)	583(3)	6·7
C(1A)	4074(2)	1388(14)	714(4)	6·0
C(2A)	4428(2)	3034(14)	463(4)	7·7
C(3A)	5024(2)	2869(11)	642(3)	4·4
C(4A)	5283(2)	928(11)	992(3)	3·7
C(5A)	4920(3)	−797(13)	1203(5)	7·8
C(6A)	4324(3)	−686(13)	1009(4)	6·8
C(7A)	5936(3)	759(15)	1189(4)	6·5
C(8A)	6306(3)	2490(14)	986(4)	5·7
C(9A)	6899(3)	2443(15)	1204(4)	5·8
C(10A)	7130(3)	504(16)	1574(3)	5·4
C(11A)	6785(3)	−1302(16)	1749(4)	7·3
C(12A)	6189(3)	−1204(16)	1540(4)	7·6
C(13A)	8056(3)	−1255(13)	1543(3)	4·0
C(14A)	8693(3)	−954(15)	1781(4)	5·2
C(15A)	8892(3)	1022(16)	2168(4)	6·6
C(16A)	9486(3)	1145(18)	2382(4)	7·0
C(17A)	9878(3)	−538(18)	2221(4)	7·4
C(18A)	9656(4)	−2428(19)	1836(6)	10·3
C(19A)	9072(4)	−2693(16)	1607(4)	7·7
C(21A)	10524(3)	−372(29)	2483(5)	9·7
C(22A)	10887(4)	−131(24)	1978(7)	11·6
C(23A)	11520(7)	−105(37)	2368(10)	16·6

Table 3 (*continued*).

Atom	*x*	*y*	*z*	B_{eq}/Å^2†
C(24A)	11726(17)	−2247(92)	2695(19)	15·0(12)‡
C(24A′)	11915(17)	−2003(92)	2311(18)	15·4(12)‡
C(25A)	10745(6)	2148(36)	1569(8)	14·3
C(31A)	3228(4)	3459(18)	362(4)	6·7
C(32A)	2584(4)	3304(24)	394(5)	9·9
C(33A)	2287(4)	5673(23)	247(6)	9·3
C(34A)	1631(4)	5561(22)	172(4)	8·2
C(35A)	1305(4)	7835(26)	−25(6)	10·6
C(36A)	658(5)	7430(29)	−200(7)	12·4
O(1B)	7148(2)	7637(13)	3767(3)	6·9
O(2B)	7271(2)	4164(11)	3234(3)	6·8
O(3B)	11529(2)	3247(15)	4324(3)	8·1
C(1B)	10913(3)	3536(13)	4279(4)	6·1
C(2B)	10668(3)	5369(16)	3880(4)	7·7
C(3B)	10072(3)	5643(13)	3807(4)	6·4
C(4B)	9709(3)	3869(14)	3980(4)	6·4
C(5B)	9972(3)	2028(17)	4370(5)	8·6
C(6B)	10571(3)	1735(13)	4487(3)	5·4
C(7B)	9067(2)	4017(11)	3804(3)	3·8
C(8B)	8816(2)	5927(11)	3430(3)	4·4
C(9B)	8216(3)	6075(13)	3268(4)	5·2
C(10B)	7868(3)	4277(13)	3444(4)	6·3
C(11B)	8109(3)	2334(13)	3807(5)	7·8
C(12B)	8710(3)	2170(13)	3956(4)	6·3
C(13B)	6943(4)	5993(17)	3429(5)	7·8
C(14B)	6331(3)	5695(13)	3196(4)	5·1
C(15B)	5952(3)	7440(15)	3359(4)	6·8
C(16B)	5357(2)	7250(14)	3168(4)	5·6
C(17B)	5142(3)	5345(16)	2765(4)	6·0
C(18B)	5515(3)	3591(15)	2599(4)	6·5
C(19B)	6104(3)	3795(13)	2809(4)	5·3
C(21B)	4500(3)	5164(23)	2493(5)	8·2
C(22B)	4162(4)	3129(31)	2867(7)	12·2
C(23B)	3529(6)	3000(45)	2472(10)	14·3
C(24B)	3213(15)	1045(68)	2543(17)	10·9(9)‡
C(24B′)	3301(19)	4780(91)	2861(20)	8·4(10)‡
C(24B″)	3198(34)	4443(187)	2460(43)	17·1(30)‡
C(25B)	4253(6)	3371(42)	3569(6)	15·1
C(31B)	11820(4)	1113(23)	4586(6)	9·8
C(32B)	12438(3)	1318(21)	4552(4)	7·6
C(33B)	12778(4)	−938(20)	4748(5)	8·2
C(34B)	13433(4)	−662(27)	4815(6)	10·8
C(35B)	13705(5)	−2932(27)	5118(8)	12·8
C(36B)	14352(4)	−2649(38)	5110(7)	15·4

† $B_{eq} = (4/3)\sum_{ij} \beta_{ij}(\mathbf{a}_i \cdot \mathbf{a}_j)$.

‡ Isotropic temperature factors. Occupation factors were fixed at 0·5 for C(24A) and C(24A′), 0·4 for C(24B), 0·3 for C(24B′) and C(24B″).

3. Results and discussion

3.1. *Polymorphism*

DSC curves of III-6T and III-6M are shown in figure 1. Both curves have broad peaks around 60–70°C, in spite of no observable change in the appearance of the crystals on microscopic observation. Figure 2 shows the temperature dependence of the powder X-ray diffraction patterns. The pattern (i) of III-6M changes gradually in the temperature range of the broad peak of DSC. With increase in temperature, the peak for the long spacing of 17 Å becomes smaller, while a new peak with a long spacing of 20 Å appears and grows up. The higher angle pattern also varies in shape. At the temperature above the DSC peak, a new pattern (iv) is produced. The pattern (v) of III-6T also changes gradually into the pattern (iv) with increase in temperature. When the incompletely changed samples were held at room temperature, the original pattern of III-6M or III-6T recovered very slowly (50 per cent/day), although the change stopped after several days and the peaks of the high-temperature phase did not vanish completely. This indicates that the transitions are essentially reversible. For the completely changed samples, however, the patterns were almost constant at room temperature.

The powder specimen precipitated rapidly from ethanol showed the pattern of figure 2 (iv). A DSC curve of the powder specimen is also given in figure 1. The curve shows no peaks below the crystal–mesophase transition temperature. It is concluded that the crystals III-6T and III-6M transform to the same high-temperature crystalline phase, which appears as a metastable state at room temperature.

The crystal–mesophase transition occurs at the second peak at 88°C, which is followed by a small peak. Thus, the high-temperature crystalline phase transforms to S_C^* via a higher ordered smectic. This feature agrees with the reported result [9]. Although the peak separation is quite insufficient, the third peak seems to be very small and the relative heights of the second and third peaks are very similar to those of cryst.–S_I^* and S_I^*–S_C^* transition peaks of III-7M. Therefore, the higher ordered smectic between the high-temperature crystalline phase and S_C^* is tentatively assumed to be S_I^*.

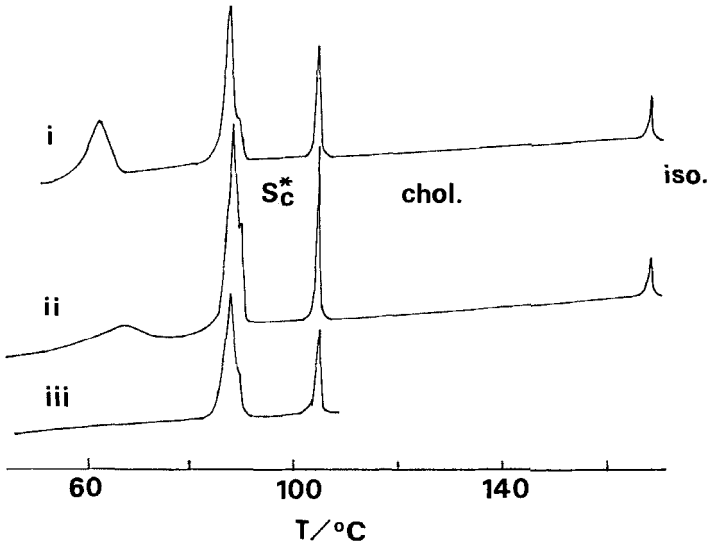

Figure 1. DSC curves. (i) III-6M, (ii) III-6T and (iii) metastable specimen.

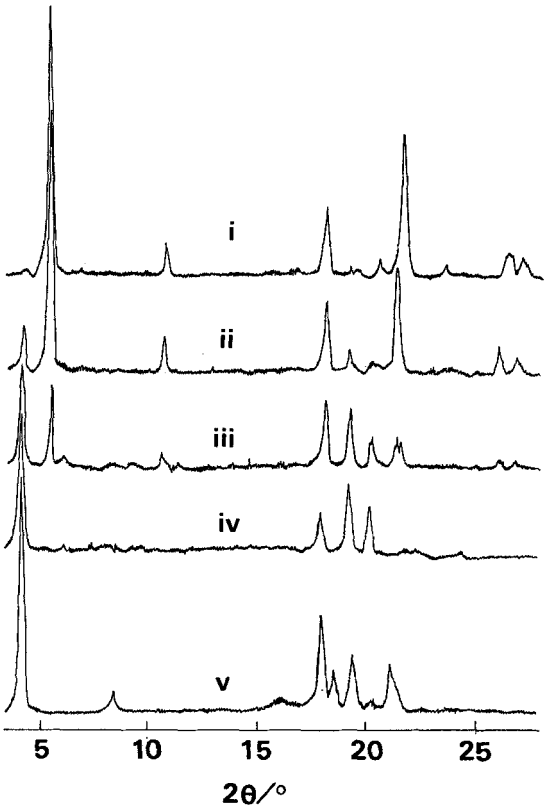

Figure 2. Powder X-ray diffraction patterns. (i) III-6M at room temperature, (ii) III-6M at 58°C, (iii) III-6M at 61°C, (iv) III-6M at 75°C and (v) III-6T at room temperature.

3.2. *Crystal structure of III-6T*

The crystal data of III-6T resemble those of III-7T, i.e. triclinic, P1, $a = 13{\cdot}37(2)$, $b = 22{\cdot}96(2)$, $c = 10{\cdot}213(5)$ Å, $\alpha = 105{\cdot}55(5)$, $\beta = 105{\cdot}22(5)$, $\gamma = 102{\cdot}31(9)°$, $V = 2775(5)$ Å^3, $z = 4$, $d_x = 1{\cdot}102$ g cm^{-3}. Moreover, similar powder X-ray diffraction patterns are obtained for both crystals, as shown in figure 3. These facts indicate that III-6T is approximately isomorphous with III-7T, which transforms to S_J^*. In the case of III-6T, the direct transition of III-6T to S_J^* is interpreted to be hidden by the intervention of the higher-temperature crystalline phase, which transforms to S_I^*.

The crystal structure is shown in figure 4. There are four crystallographically independent molecules, A, B, C, and D. The molecules have twisted biphenyl moieties, whose dihedral angles are 21° (A), 36° (B), 42° (C), and 13° (D). All the paraffin chains have twisted conformations (table 4) and those of the molecules, A, C and D are highly disordered. Chiral groups of these molecules are also disordered. The ORTEP drawings [10] of the molecules A and B are shown in figure 5.

The crystal has a smectic-like layer structure in which parallel pairs, A–C and B–D, have an antiparallel arrangement. The layer plane is parallel to the *ac* plane, to which the molecular long axis is tilted with an angle of 45°. Some of the mutual arrangements of the nearest phenyl rings between the neighbouring molecules are nearly parallel; i.e. 27° (A(i)–B(iii)), 6° (A(iii)–D(ii)), 28° (A(iii)–C(ii)), 6° (B(ii)–C(ii)), 20° (B(ii)–D(iii)), and 22°

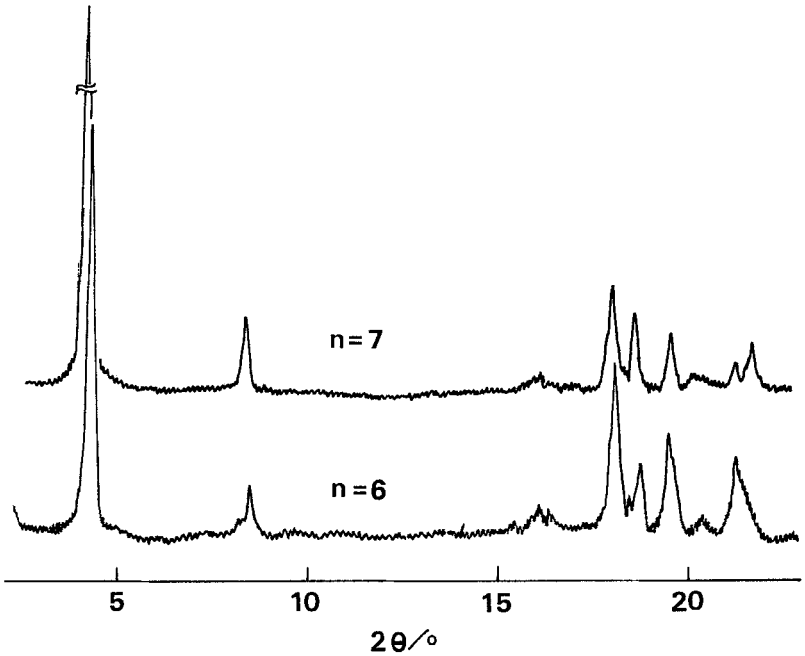

Figure 3. Powder X-ray diffraction patterns of III-7T (upper) and III-6T (lower).

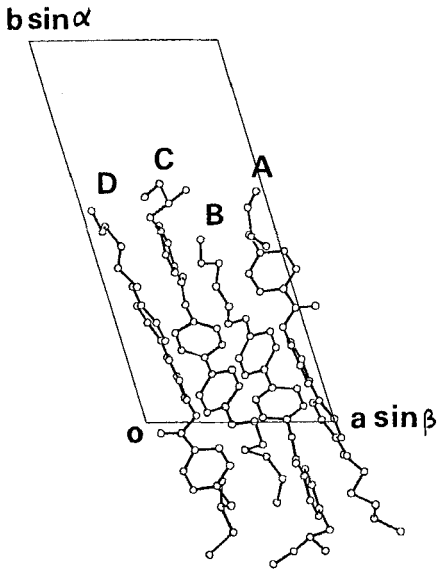

Figure 4. The crystal structure of III-6T viewed along the *c* axis. Disordered atoms with minor occupancies are omitted for simplicity. The molecular long axis tilts to the direction nearly perpendicular to the paper sheet with an angle of 45°.

Table 4. Tortion angles (ϕ/°) of paraffin chains.

	III-6T				III-6M	
	Mol. A	Mol. B	Mol. C	Mol. D	Mol. A	Mol. B
O3–C31–C32–C33	−98	−89	−62	55	−173	174
C31–C32–C33–C34	175	168	−175	171	−172	171
C32–C33–C34–C35	100	86	48	−28	176	−171
C33–C34–C35–C36	154	165	167	−167	−170	−175

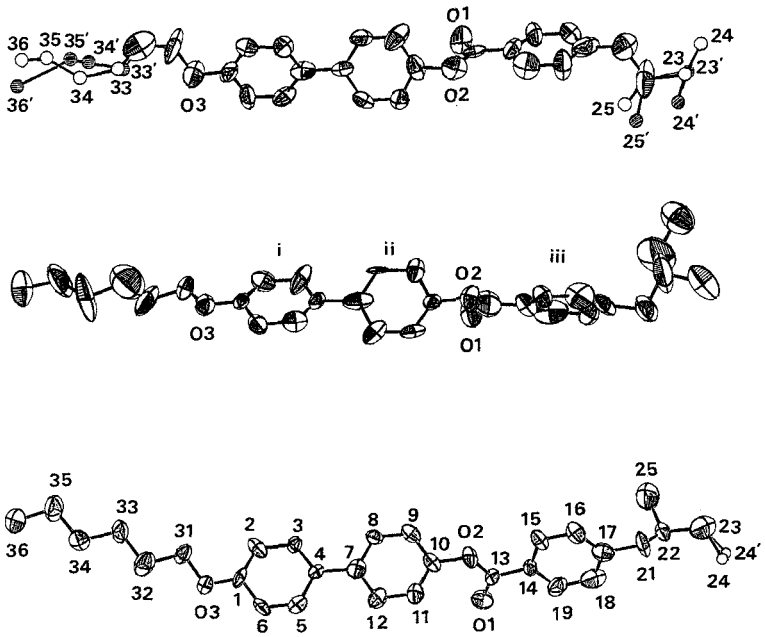

Figure 5. ORTEP drawings of the molecules A (upper), B (middle) of III-6T, and A of III-6M (lower) with 50 per cent probability thermal ellipsoids. The molecules C and D of III-6T have similar core moieties with those of the molecules B and A of III-6T, respectively, and high disordered chains. The molecule B of III-6M is almost the same as the molecule A of III-6M. Isotropically refined atoms are shown by spheres with an arbitrary diameter. All the molecules are numbered in the same way.

(C(iii)–D(i)), where (i), (ii) and (iii) are the numbering of the phenyl rings as shown in figure 5. In contrast, all of the other crystals determined by us, which transform to S_C^* or S_I^*, have contacts with the angle of about 60° [2–4]. This was interpreted that the molecular rotation would be easily induced at the crystal–mesophase transition. In the present case, the nearly parallel arrangements of the phenyl rings mentioned previously suggest difficulty of free rotation of molecules along their long axes, because hydrogen atoms of the phenyl rings are interdigitated, as is shown in figure 6. Therefore, this feature is closely related to the highly ordered structure of S_J^*.

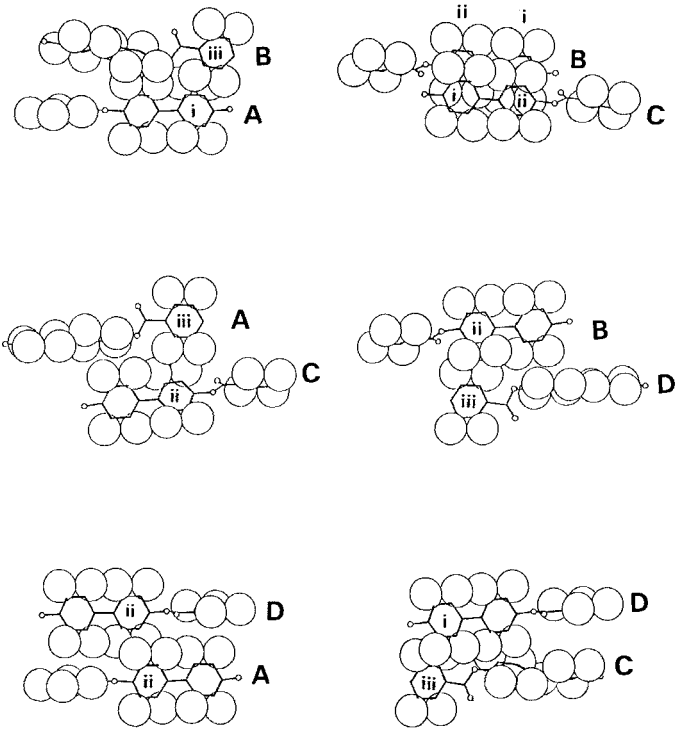

Figure 6. Mutual arrangements of the phenyl rings in the III-6T crystal. Hydrogen atoms are drawn with the C–H distance of 1·0 Å and the van der Waals radius of 1·2 Å.

3.3. *Crystal structure of III-6M*

As mentioned previously, III-6M does not transform directly to a mesophase. Nevertheless, it is expected to be useful to know and compare the polymorphic structures with each other in order to understand the intermolecular interaction, since a molecular packing mode in a stable crystal lattice results from a balance of the various kinds of intermolecular interactions.

The crystal structure of III-6M is shown in figure 7. There are two crystallographically independent molecules, A and B, which are related by a pseudo-inversion. The ORTEP drawing of one of the molecules is shown in figure 5. Molecules have approximately coplanar biphenyl moieties (4·9° for A and 4·4° for B) and almost all-trans zigzag paraffin chains (table 4). The C(24) atoms of the chiral groups are disordered.

The crystal has a smectic-like layer structure composed of an antiparallel arrangement of the two independent molecules. The layer plane is parallel to the $(10\bar{1})$ plane. The molecular long axis is largely tilted (60°) in the layer. The contact angle of the nearest phenyl rings between adjacent molecules is 60° on average. Ester groups are in proximity with the antiparallel arrangement between the adjacent molecules.

These aspects are quite different from those of III-6T and III-7M, but rather similar to those of the crystals of the series I, which are closely related to S_C^* followed by a cholesteric. This may be interpreted as follows: although the ester–ester interaction is dominant in III-6M, the ester–ether association would be also realized in this crystal by

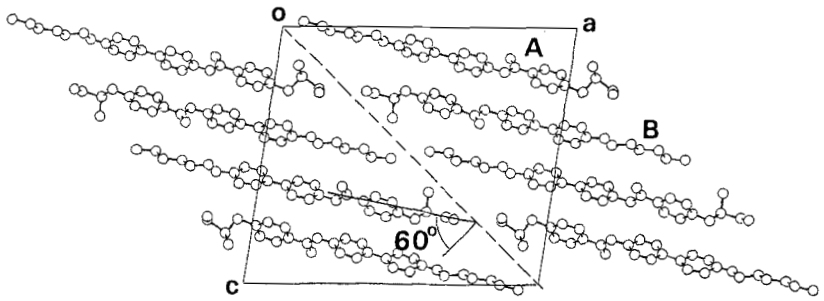

Figure 7. The crystal structure of III-6M viewed along the *b* axis. The broken line denotes a layer plane.

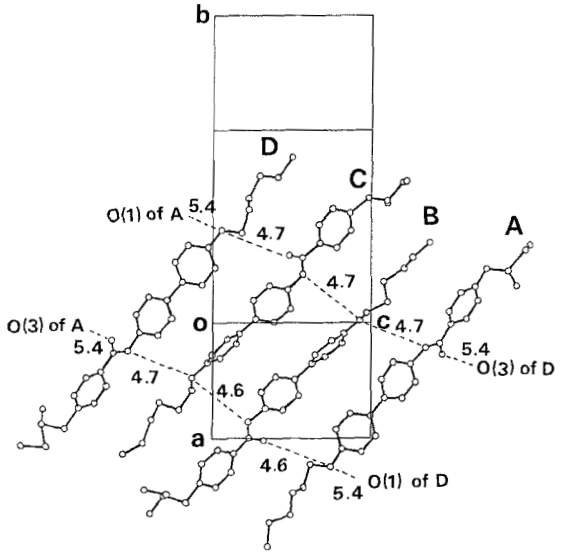

Figure 8. O–O distances (Å) in III-6T.

a slight translation of molecules along the molecular long axis, since the ester–ether distance is rather short (O(1)–O(3), 4·5 Å; O(2)–O(3), 5·7 Å). This translation causes lengthening of the long spacing. Thus, it is assumed that the transition from III-6M to the high-temperature crystalline phase would be accompanied by the translation, because the long spacing becomes longer at the transition. On the other hand, in III-6T, the ester–ether interaction is dominant; linear chains of comparable O–O distances to those of III-6M between the ester and ether groups are observed along [102], as shown in figure 8. If the two modes of the arrangements of the polar groups are competitive in this compound, the ester–ester association would be realized again at the S_I^*–S_C^* transition. Thus, the resemblance of the structure of III-6M to those of the series I crystals is related to the common feature of these compounds of having a S_C^* phase which transforms not to S_A but to a cholesteric. A slight difference is, however, found between the series I crystals and III-6M. The close inter-chain contacts between layers as observed in the series I crystals are not found in III-6M. The layer plane is clearer than that in the series I, indicating that the interlayer interaction is much weaker than in the series I crystals.

It is concluded that the subtle balance of intermolecular interactions brings out polymorphs with quite different crystal structures, which are related to different mesophase characteristics.

References

[1] For $n=5$, S_C^* appears only monotropically.
[2] HORI, K., and OHASHI, Y., 1988, *Bull. chem. Soc. Japan*, **61**, 3859.
[3] HORI, K., TAKAMATSU, M., and OHASHI, Y., 1989, *Bull. chem. Soc. Japan*, **62**, 3859.
[4] HORI, K., and OHASHI, Y., 1989, *Bull. chem. Soc. Japan*, **62**, 3216.
[5] MAIN, P., HULL, S. E., LESSINGER, L., GERMAIN, G., DECLERCQ, J.-P., and WOOLFSON, M. M., 1978, MULTAN78. A system of computer programs for the automatic solution of X-ray diffraction data, University of York, England and University of Louvain, Belgium.
[6] SHELDRICK, G. M., 1976, SHELX76. A program for crystal structure determination, University of Cambridge.
[7] IBERS, J. A., and HAMILTON, W. C. (editors), 1974, *International Tables for X-ray Crystallography*, Vol. IV (Kynoch Press).
[8] The tables of the bond lengths and angles, anisotropic temperature factors of the non-hydrogen atoms, the atomic parameters for hydrogen atoms and the F_o-F_c list have been deposited as a Supplementary Publication, comprising 28 pages with the British Library Document Supply Centre. Copies may be obtained by using the procedure described at the end of this issue and by quoting SUP 16518.
[9] GOODBY, J. W., and LESLIE, T. M., 1984, *Molec. Crystals liq. Crystals*, **110**, 175.
[10] JOHNSON, C., 1965, ORTEP. Report ORNL-3794, Oak Ridge National Laboratory, Tennessee.